Geophysical Research Letters

RESEARCH LETTER
10.1029/2022GL101084

Division of Magnetic Flux Rope via Magnetic Reconnection Observed in the Magnetotail

Xinmin Li[1,2,3], **Rongsheng Wang**[1,2,3], **and Quanming Lu**[1,2,3]

[1]Deep Space Exploration Laboratory, School of Earth and Space Sciences, University of Science and Technology of China, Hefei, China, [2]CAS Center for Excellence in Comparative Planetology, CAS Key Laboratory of Geospace Environment, Anhui Mengcheng National Geophysical Observatory, University of Science and Technology of China, Hefei, China, [3]Collaborative Innovation Center of Astronautical Science and Technology, Harbin, China

Key Points:

- An electron diffusion region of reconnection is observed at the center of the flux rope (FR) in the magnetotail
- The reconnecting current layer can change the magnetic field topology inside the FR and divide it into two secondary FRs
- The Hall magnetic field inside the reconnecting current layer leads to the crater-shaped magnetic field magnitude within the FR

Correspondence to:
R. Wang,
rswan@ustc.edu.cn

Citation:
Li, X., Wang, R., & Lu, Q. (2023). Division of magnetic flux rope via magnetic reconnection observed in the magnetotail. *Geophysical Research Letters*, *50*, e2022GL101084. https://doi.org/10.1029/2022GL101084

Received 31 AUG 2022
Accepted 13 DEC 2022

Abstract Using high-resolution data from Magnetospheric Multiscale (MMS) mission, we report an intense current layer at the center of a flux rope (FR) in the magnetotail. The intense current layer is caused by the compression of the ion bulk flows at the center of a FR rather than two interlaced flux tubes reported at the magnetopause previously. The intense current layer has been identified as an electron diffusion region of the magnetic reconnection, and the hall magnetic field generated by magnetic reconnection makes the FR show crater-shaped. The reconnecting current layer is supported by the poloidal magnetic field of the FR, and it is dividing the FR into two secondary FRs. The observations suggest that magnetic FR can be compressed easily to excite instability inside it as it is propagating in the magnetotail current sheet, thus changing its magnetic topology.

Plain Language Summary Magnetic flux ropes (FRs) consist of a poloidal magnetic field and an axial magnetic field component and are always described as helical magnetic field structures. The FRs play an important role in particle acceleration, magnetic flux transportation, and the evolution of reconnection. Recently, with high-resolution magnetic field and plasma moments measurements, it is found that the interior of the FR is active, and a lot of processes could occur therein. In this work, we report a FR embedded in an unstable tailward plasma flow in the magnetotail. An ongoing reconnection current layer is observed at the center of the FR. The reconnecting current layer could change the magnetic field topology of the initial FR and divide the initial FR into two secondary FRs.

1. Introduction

Magnetic flux ropes (FRs) are helical magnetic field structures consisting of a poloidal magnetic field and an axial magnetic field component, which have been frequently observed in the terrestrial magnetosphere, such as magnetopause (Deng & Matsumoto, 2001; Eastwood et al., 2016; Hwang et al., 2016; Russell & Elphic, 1978; J. Zhong et al., 2013), magnetotail (Sibeck et al., 1984; Slavin et al., 2003; R. S. Wang, Lu, Du, & Wang, 2010; Zhao, Wang, & Du, 2016; Zong et al., 2004), and magnetosheath (Z. Z. Chen et al., 2019; S. Y. Huang et al., 2016; S. M. Wang et al., 2021; Yao et al., 2020). As one FR passes through the spacecraft, its typical signature is a bipolar variation of the poloidal magnetic field component with an enhancement of the axial magnetic field component. FRs are always observed around the diffusion region of magnetic reconnection (Russell & Elphic, 1978; Slavin et al., 2003; Teh et al., 2017; R. S. Wang, Lu, Du, & Wang, 2010), and are supposed to be generated by magnetic reconnection (Eastwood et al., 2005; Hasegawa et al., 2010; Lee & Fu, 1985; M. Øieroset et al., 2011; Russell & Elphic, 1978; Scholer, 1988). Meanwhile, the FRs play an important role in the process of magnetic reconnection, such as accelerating electrons (L. J. Chen et al., 2008; Drake et al., 2006; Fu et al., 2006; R. S. Wang, Lu, Li, et al., 2010; Xia & Zharkova, 2018; Z. H. Zhong et al., 2020), accomplishing fast reconnection (Bhattacharjee et al., 2009; Daughton et al., 2009; Loureiro et al., 2007; Samtaney et al., 2009), and dominating the reconnection evolution (Daughton et al., 2011; R. S. Wang et al., 2016).

In the earlier literature when relatively low-time resolution spacecraft data were used, FRs were well described by a force-free model, and the current density derived from the Curlometer technique inside them was dominated by the axial component (e.g., Slavin et al., 2003). Most recently, with the high-resolution magnetic field and plasma moments data measured by Magnetospheric Multiscale (MMS) mission (Burch, Moore, et al., 2016), it was found that the current density was structured, and the current sheet fragmented into a series of filamentary currents

within the FRs (Eastwood et al., 2016; R. S. Wang et al., 2017). The thickness of the filamentary currents can be comparable to the ion scale, and even down to the electron scale. The filamentary currents were highly dynamic and were fragmenting into smaller filamentary currents (R. S. Wang et al., 2017). Furthermore, the secondary reconnection can occur inside filamentary currents within the FRs (S. M. Wang, Wang, et al., 2020), as predicted in simulations (C. Huang et al., 2017; Lapenta et al., 2015).

Another kind of current structure deviating from the force-free model was an extremely intense current sheet embedded in the background current at the center of the FR (Hasegawa et al., 2010; M. Øieroset et al., 2011; S. M. Wang et al., 2021). Also, recent observations suggest that the reconnection could occur at such a current sheet at the magnetopause (Øieroset et al., 2016). However, further analyses show that these intense reconnecting current sheets were created by two interlaced flux tubes rather than inside the center of one standard FR, because the electron pitch angle distributions (PAD) on the two sides of the intense current sheet were quite different, which indicates that the plasmas on the two sides were not magnetically connected (Hwang et al., 2020; Kacem et al., 2018; Kieokaew et al., 2020; Øieroset et al., 2019). Latest statistics show that the ubiquitous intense current sheet, where the reconnection was common, observed at the centers of the rope-like structures was caused by two interlinked flux tubes (Fargette et al., 2020).

In this paper, we report an intense current layer at the center of one FR in the magnetotail, analogous to the previous observations at the magnetopause. This intense current layer was caused by the compression of the ion bulk flows at the center of a FR rather than two interlaced flux tubes reported at the magnetopause previously. The reconnection was occurring at the intense current layer and dividing the FR into two which has never been observed. It indicates that the intense current layer can be spontaneously generated inside the FR and change its magnetic topology.

2. Instrumentation

The data used in this letter was measured by MMS (Burch, Moore, et al., 2016). The magnetic and electric fields were measured by Flux Gate Magnetometer with a time resolution of 128 Hz (Russell et al., 2016) and the electric field double probe with a time resolution of 8,192 Hz (Ergun et al., 2016; Lindqvist et al., 2016), respectively. The particle moments and distributions data were taken from Fast Plasma Investigation (FPI) (Pollock et al., 2016). The time resolution was 30 ms for electrons and 150 ms for ions. The electron Partial moments data was used to avoid the error from low density. During this event, only MMS1 and MMS2 provided the FPI data, and the measurements at them were almost the same. Thus, the data from MMS2 were used in this paper unless otherwise stated.

3. Observation and Analysis

3.1. Overview of the Flux Rope

During 16:55:00–16:57:30 UT on 02 August 2020, the MMS spacecraft was located at [−28.1, −3.6, 2.6] Re in the Geocentric Solar Ecliptic (GSE) coordinates system and detected a FR as shown in Figure 1. The plasma beta (yellow trace in Figure 1b), the ratio of thermal pressure to magnetic pressure, was greater than 1.0 in the whole interval, suggesting that the FR was located in the plasma sheet. The FR was observed between 16:55:56 and 16:56:32 UT, identified by the bipolar variation of B_z (red traces in Figure 1c) and the enhancement of the magnitude of magnetic field, dominated by the out-plane magnetic field B_y. Accompanying with B_z reversal, B_x also changed from positive to negative, suggesting that the spacecraft had crossed the cross-section center of the FR. At the center of the FR (~16:56:14.5 UT), where B_z changed from positive to negative, the magnitude of the magnetic field had a sharp depression, similar to the crater-shaped FR (Labelle et al., 1987; Zhang et al., 2010) which has a magnetic field depression at its center.

The FR was embedded in an unstable tailward ($V_{i,x} < 0$) plasma flow (Figure 1d). By assuming that the FR moved in the X direction with the average speed of the plasma flow, ~500 km/s, we roughly estimated the scale of the FR was about 2.8 R_e or 27 d_i, where d_i = 660 km is the ion inertial length based on $N = 0.12\text{cm}^{-3}$. At around the leading (tailward side) edge of the FR, the tailward plasma velocity was about −400 km/s. And then, the velocity became increasingly faster. The maximum velocity was up to −800 km/s, which appeared behind the center of the FR (~16:56:17 UT). Finally, as the trailing (earthward side) edge approached, the plasma velocity

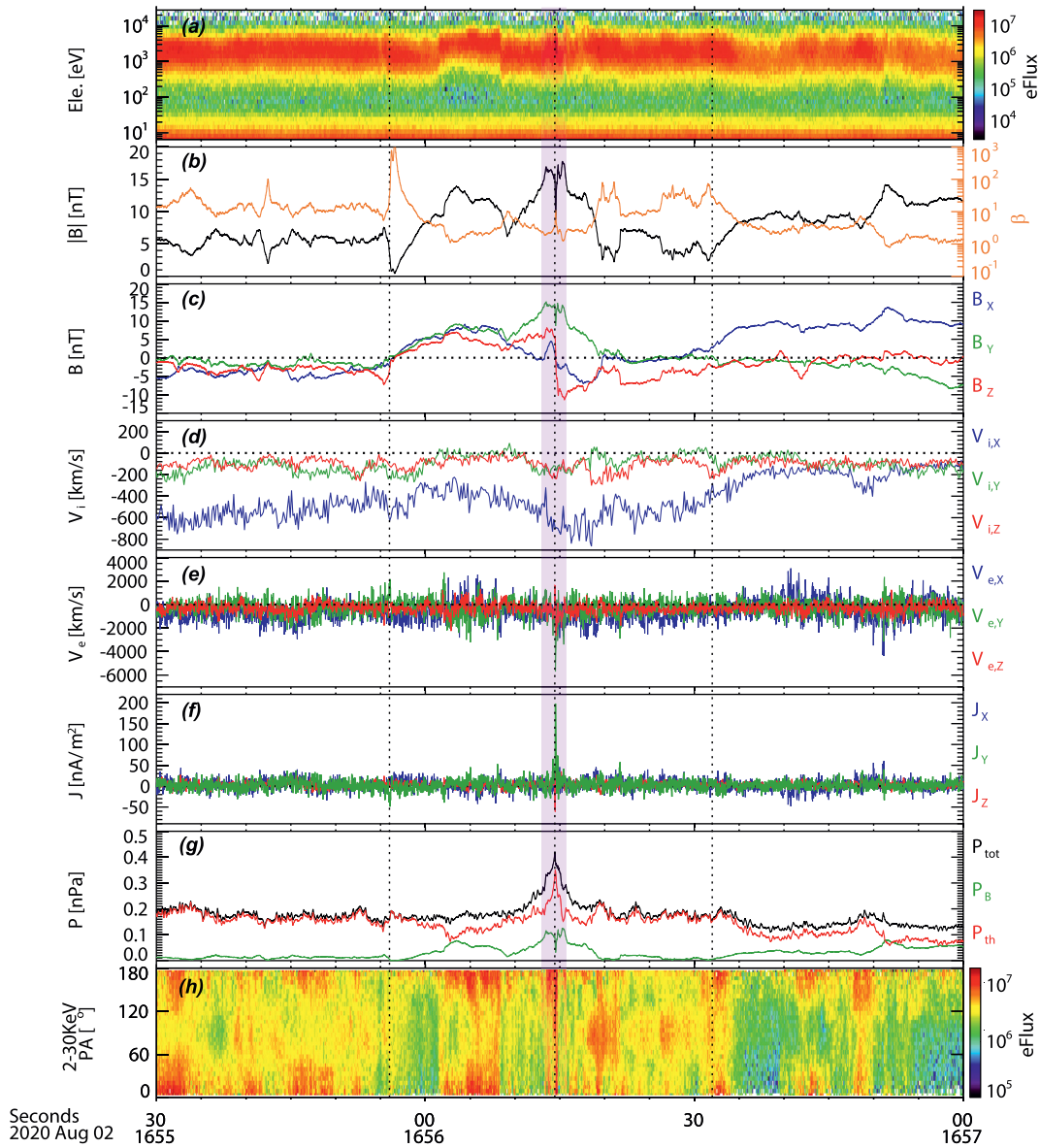

Figure 1. Overview of the flux rope in Geocentric Solar Ecliptic coordinates. (a) Electron energy spectrogram; (b) the magnitude of magnetic field (black trace) and the plasma beta (yellow trace); (c) magnetic field vector; (d) ion bulk flow; (e) electron bulk flow; (f) current density vector; (g) total (black), magnetic (blue), and plasma (red) pressure; (h) electron pitch angle distribution at energies 2–30 KeV.

gradually decreased to about −450 km/s. The velocity distribution through the FR suggested that the leading part was contracting, but the trailing part was expanding (as illustrated in Figure 4). Due to the maximum velocity appearing at the trailing side of the FR, the center of the FR was compressed as well.

The compression of the center of the FR was supported by the change of pressure, as shown in Figure 1g. Total pressure (black trace in Figure 1g) was roughly balanced at the leading edge (16:55:56–16:56:09 UT) and trailing edge (16:56:22–16:56:32 UT), but it was significantly enhanced around the center of the FR, indicating that the center of the FR was strongly compressed. The unbalanced pressure also suggested that the magnetic field lines on the two sides would continue to pour into the center of the FR (Russell & Qi, 2020). Furthermore, the magnitude of B_z (red traces in Figure 1c) on both sides of the center of the FR was enhanced just before the sign changed, indicating that the normal magnetic field with respect to the tailward flow was indeed compressed.

Due to the strong compression, an intense but narrow current layer (Figure 1f) was observed at the center of the FR. The direction of the current layer was primarily along + y axis, which was consistent with the background current of the FR. The electron PADs (Figure 1h) were volatile inside the FR. At the leading part (16:55:56–16:56:14.54 UT), the electron differential fluxes were first concentrated at around 180°, then became bidirectional field-aligned distribution, and finally concentrated at around 180° as approaching the current layer again. At the trailing part (16:56:14.54–16:56:32 UT), the electron differential fluxes were first concentrated at around 180°, and then the fluxes enhanced at around 90°, leading to the perpendicular distribution. However, it is worth noting that the PADs were not changed dramatically around the current layer (the pink region in Figure 1), as the spacecraft right passed through it. Based on the above analyses, an intense current layer was observed at the center of the FR. In the following, we will focus on this current layer, and the magnetic reconnection will be proven to be ongoing here.

3.2. Magnetic Reconnection in the Current Layer

Figure 2 shows a closer view of the reconnecting current layer in the local current coordinate system. The transformation matrix was obtained from the hybrid method. M was along the direction of maximum current density in this current layer (at 16:56:14.52 UT). N was calculated by $N = L_{\mathrm{MVA}} \times M$, where L_{MVA} was the direction of maximum variance from the minimum variance analysis (Sonnerup & Scheible, 1998) based on the magnetic field data taken from 16:56:14–16:56:15 UT. And L completed the right-handed system. The transformation matrix relative to GSE coordinates was given by $L = [0.3401, -0.0067, 0.9404]$, $M = [0.1296, 0.9908, -0.0398]$, and $N = [-0.9314, 0.1354, 0.3378]$. N was almost parallel to the normal direction of the current layer obtained from the timing method (Schwartz, 1998), with a small deviation of 8°. The timing method was also used to calculate the velocity of the current layer, which was calculated to be 775 km/s along the $+N$ direction. The duration of the current layer crossing was about 0.22s (16:56:14.43–16:56:14.65 UT) (Figure 2f), so its thickness was estimated about 170 km ~ 11 d_e, where the electron inertial length d_e = 15 km, based on $N_e = 0.12$ cm^{-3}.

Figure 2b shows the three components of the magnetic field. The reconnecting magnetic field $\boldsymbol{B}_L$ changed from positive (~+9 nT) to negative (~−10 nT). At 16:56:14.54 UT, when $\boldsymbol{B}_L = 0$, $\boldsymbol{B}_N$ had a small but positive value of ~3 nT, suggesting that the spacecraft crossed the reconnecting current layer on the $+\boldsymbol{L}$ side of the X-line. Meanwhile, there was a significant decrease in $\boldsymbol{B}_M$ by ~5 nT from the background value of 14 nT. The background $\boldsymbol{B}_M$ was around 1.4 times as large as the reconnecting component $\boldsymbol{B}_L$, indicating that the reconnection current layer had a strong guide field. The electric field E_N (Figure 2e) showed a bipolar variation from negative to positive and always pointed into the center of the current layer on both sides, consistent with the Hall electric field.

Ions bulk flows (Figure 2c) remained constant throughout the current layer. Different from ions, two reversed electron jets were visible in $V_{e,L}$ at around 16:56:14.46 and 16:56:14.58 UT (Figure 2d). The magnitudes of these reversed jets were almost equal and $|\delta V_{e,L}| \sim$ 2,000 km/s relative to the background electron bulk flow of about −1,000 km/s. They were much larger than the local ion Alfven speed (V_a = 630 km/s, based on the B_0 = 10 nT, and Ne = 0.12 cm^{-3}). The two reversed electron jets respectively corresponded to the electron outflow (positive jet) and inflow (negative jet) of the reconnection current layer (illustrated in Figure 4), and they resulted in the decrease of $\boldsymbol{B}_M$, corresponding to the Hall magnetic field. A unipolar Hall magnetic field was observed here, consistent with the simulations (Huba, 2005; Pritchett & Coroniti, 2004; Ricci et al., 2004), where the reconnection current sheet with a strong guide field could just produce the unipolar Hall magnetic field. Based on the magnetic field, electric field, and electron bulk flow, a reconnecting current layer was identified at the center of the FR, as illustrated in Figure 4.

3.3. Signatures of Electron Diffusion Region

The current layer was mainly supported by the intense electron flow $V_{e,M}$ (Figures 1e and 2d), indicating that the spacecraft should be in or near the electron diffusion region (EDR). Figure 2g shows the comparison between E_N and $-(V_e \times B)_{\mathrm{N}}$, and they were different around the center of the current layer (16:56:14.43–16:56:14.65 UT), suggesting that electrons were decoupled from magnetic fields. The parallel ($T_{e,\parallel}$) and perpendicular ($T_{e,\perp}$) electron temperatures were shown in Figure 2h. $T_{e,\parallel}$ was much larger than $T_{e,\perp}$, apart from the center of the current layer. At the center of the current layer, $T_{e,\perp}$ increased significantly and was equaled to $T_{e,\parallel}$. The characteristics of

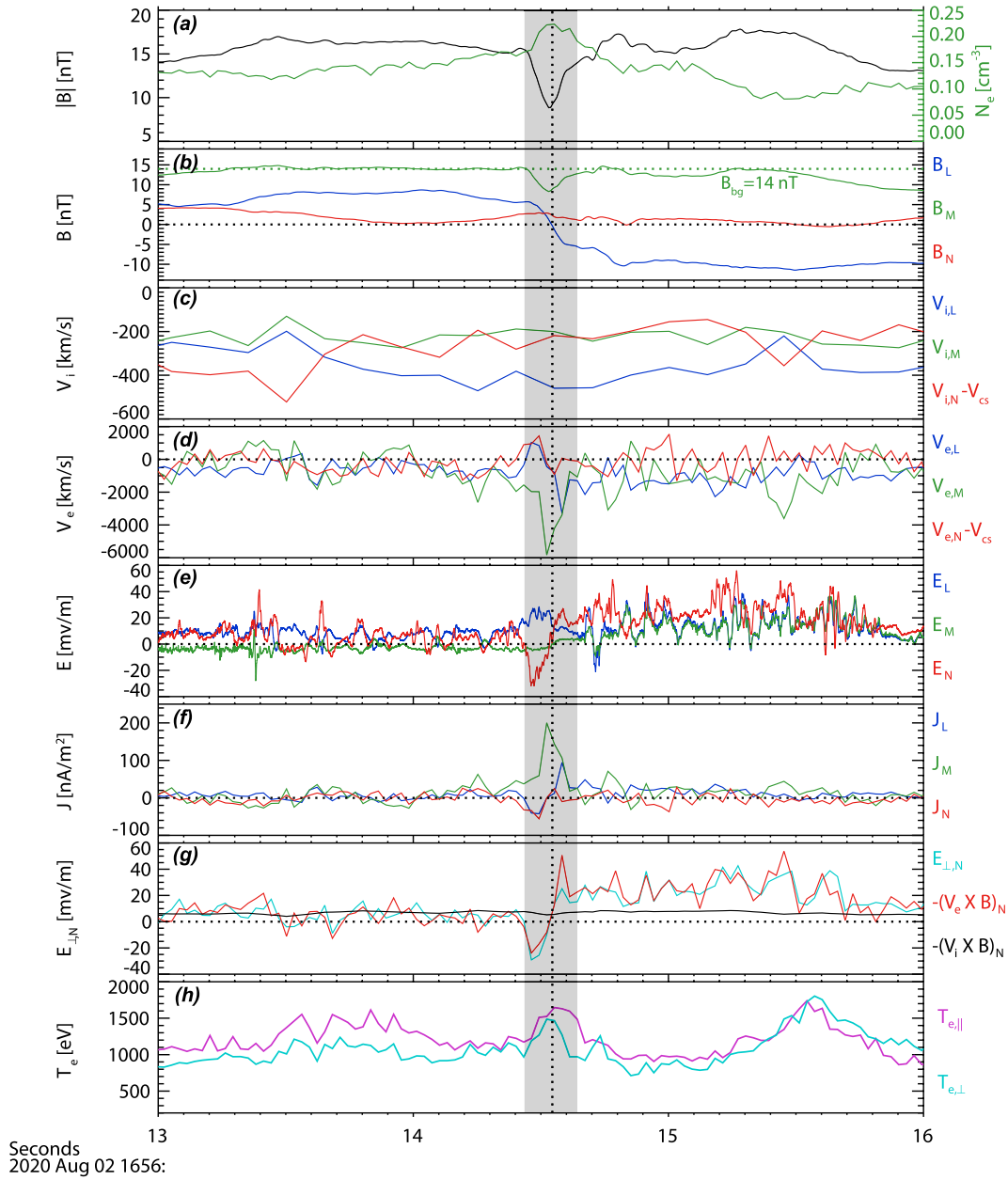

Figure 2. Closer view of the reconnecting current layer in LMN coordinates. (a) |B| (black trace) and N_e (green trace); (b) magnetic field vector; (c) ion bulk flow; (d) electron bulk flow; The velocity of the current layer (V_{cs}) obtained from timing method has been subtracted from the ion and electron bulk flow. (e) Electric field vector; (f) current density vector; (g) $\mathbf{E}_{\perp,N}$, $-(\mathbf{V}_i \times \mathbf{B})_N$, and $-(\mathbf{V}_e \times \mathbf{B})_N$; (h) $T_{e,\|}$ (magenta trace) and $T_{e,\perp}$ (cyan trace).

electron temperature were consistent with the previous observations in the EDR (Burch, Torbert, et al., 2016; Li et al., 2019; Torbert et al., 2018; R. S. Wang, Lu, et al., 2020).

In order to further establish the EDR encounter, multiple spacecraft observations for the crossing of the current layer were shown in Figure 3. Four MMS spacecraft had similar but time-shifted variations in $\boldsymbol{B}_L$ (Figure 3a). The reversal points of $\boldsymbol{B}_L$ (the center of the current layer) were observed by MMS2, MMS4, MMS3, and MMS1 in turn, consistent with the spatial distribution of four spacecraft in the $\boldsymbol{N}$ direction (Figure 3h). The unipolar Hall magnetic field, the decrease of $\boldsymbol{B}_M$, was observed by four spacecraft (Figure 3b). All four spacecraft observed the positive enhancement of the normal magnetic field $\boldsymbol{B}_N$ (Figure 3c), indicating that all of them crossed the $+\boldsymbol{L}$ side of the X-line. Considering the spatial distribution of four spacecraft in the $\boldsymbol{L}$ direction (Figure 3h), MMS3 should

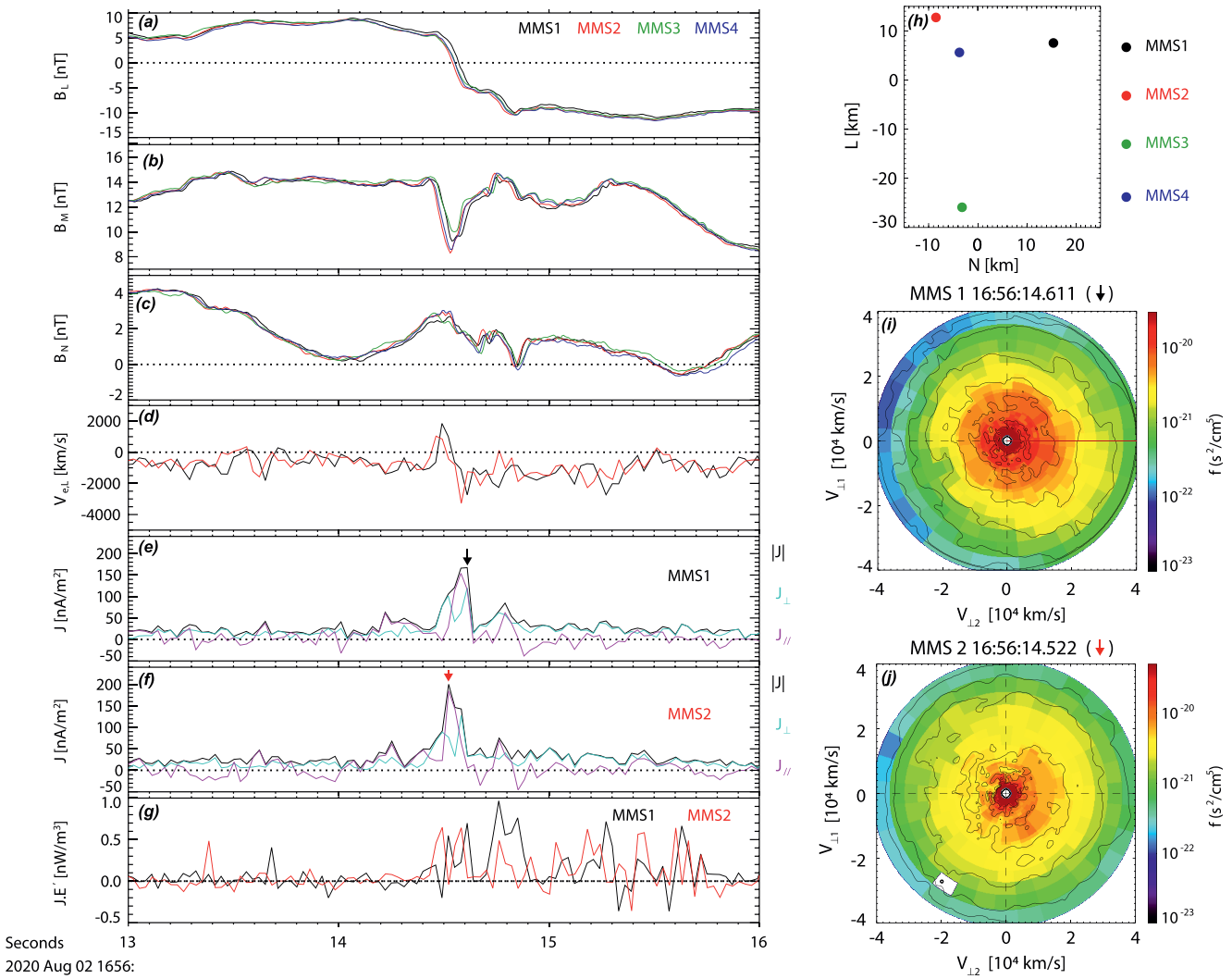

Figure 3. Multiple spacecraft observations of the reconnection current layer. (a–c) three components of the magnetic field observed by four spacecraft; (d) $V_{e,L}$ observed by Magnetospheric Multiscale 1 (MMS1) (black trace) and MMS2 (red trace); (e–f) current density in field-aligned coordinates measured by MMS1 and MMS2; (g) $\mathbf{J} \cdot (\mathbf{E} + \mathbf{V}_e \times \mathbf{B})$ measured by MMS1 (black trace) and MMS2 (red trace); (h) location of MMS spacecraft in the L-N plane; (i) and (j) electron velocity distributions in perpendicular plane measured by MMS1 and MMS2, $\mathbf{V}_{\perp 1} = (\mathbf{b} \times \mathbf{v}) \times \mathbf{b}$ and $\mathbf{V}_{\perp 2} = (\mathbf{b} \times \mathbf{v}) \times \mathbf{b}$, where $\mathbf{b}$ and $\mathbf{v}$ are unit vectors of $\mathbf{B}$ and $\mathbf{V}_e$.

be closest to the X point. However, there was no FPI data available from MMS3 and MMS4 for this time interval, so the particle data only from MMS1 and MMS2 were shown in Figure 3.

Because MMS1 and MMS2 were close in the $\boldsymbol{L}$ direction, the reversed electron jets were observed by both MMS1 and MMS2, and the magnitudes were similar (Figure 3d). Figures 3e and 3f show the current density in field-aligned coordinates measured by MMS1 and MMS2, respectively. The difference between the two spacecraft was negligible. The parallel current $J_{\parallel}$ had obvious enhancements and was greater than the perpendicular current $J_{\perp}$ at the center of the current layer, which was consistent with the observation of EDR (R. S. Wang, Lu, et al., 2020). Energy dissipation rates in the electron rest frame $\mathbf{J} \cdot (\mathbf{E} + \mathbf{V}_e \times \mathbf{B})$ (Zenitani et al., 2011) measured by MMS1 (black trace) and MMS2 (red trace) were simultaneously displayed in Figure 3g. There were significant positive $\mathbf{J} \cdot (\mathbf{E} + \mathbf{V}_e \times \mathbf{B})$ around the center of the current layer, suggesting the magnetic energy was transferred to the plasma here. Furthermore, the strong energy dissipation was also observed behind the center of the current layer (16:56:14.7–16:56:15.8 UT), which may be related to the large-amplitude fluctuations of the electric field during this period (Figure 2e).

Figures 3i and 3j show the electron velocity distributions in the perpendicular plane measured by MMS1 and MMS2 at the center of the current layer, denoted by the black and red arrows in Figures 3e–3f, respectively. The

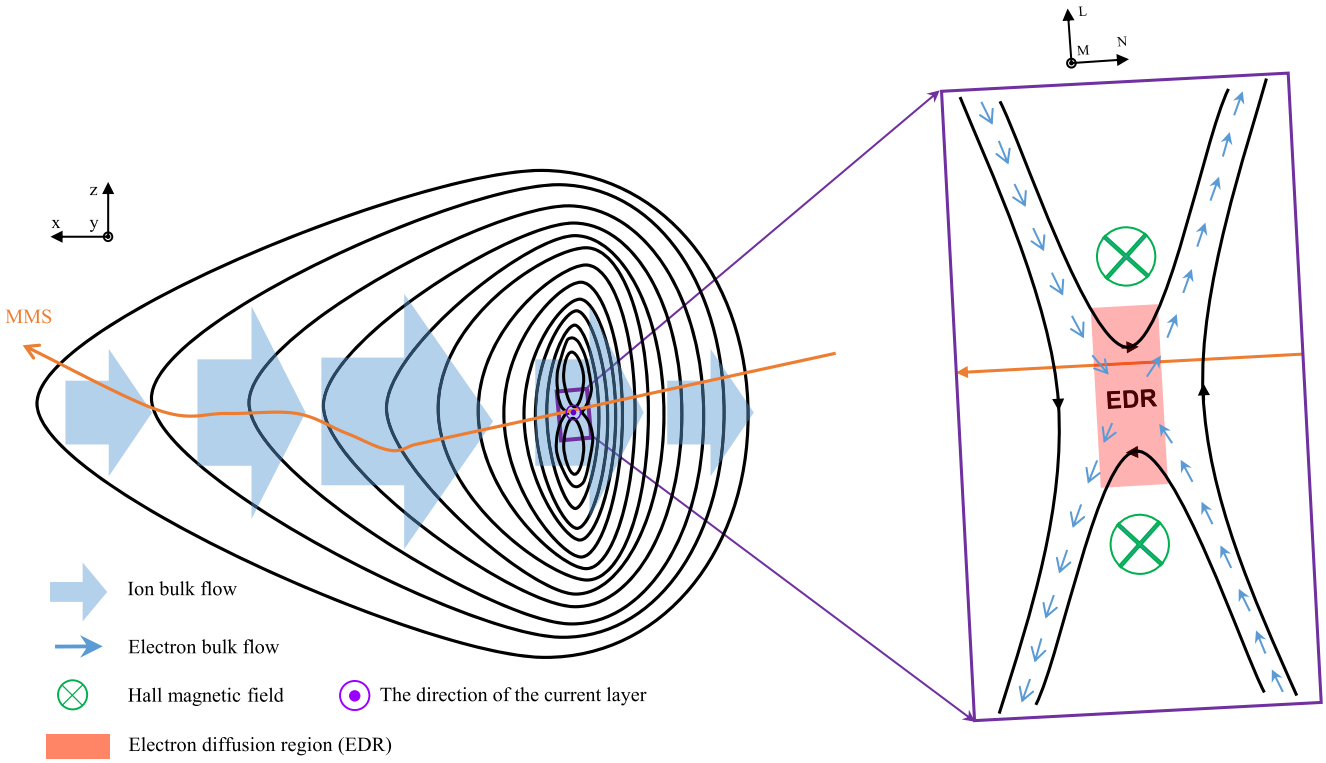

Figure 4. A schematic illustration for the flux rope and the reconnecting current sheet at its center.

crescent-shaped distributions were observed by both MMS1 and MMS2, which were similar to the typical electron velocity distributions of the EDR (Burch, Torbert, et al., 2016; Li et al., 2019; Torbert et al., 2018). Based on the above, it can be concluded that the spacecraft encountered the EDR.

4. Discussion and Conclusions

In this paper, we report a crater-shaped FR embedded in an unstable tailward plasma flow in the magnetotail. Due to the unstable plasma flow, the center of the FR was strongly compressed. Thus, a reconnecting current layer with a strong guide field formed at the center of the FR, and the reconnecting magnetic field was dominated by the poloidal magnetic field (B_z) of the FR. The central intense current layer was identified as the EDR, characterized by electron demagnetization, positive energy dissipation, and agyrotropic crescent-shaped electron velocity distributions.

The reconnecting current sheets occurring at the center of the rope-like structures, characterized by the bipolar variation of the magnetic field component and the enhancement of the magnitude of the magnetic field, have been observed at the magnetopause (Fargette et al., 2020; Hwang et al., 2020; Kacem et al., 2018; Kieokaew et al., 2020; M. Øieroset et al., 2016; M. Øieroset et al., 2019). However, these rope-like structures have been interpreted as two interlinked flux tubes instead of FRs. Because the electron PADs showed rapid change as the spacecraft right passed through the current sheet, and the bipolar signature of the FR was not observed in the component normal to the magnetopause (X-GSE), which deviated from the regular FR observed at the magnetopause (Kacem et al., 2018). In this paper, a similar phenomenon was first observed in the magnetotail. In contrast, although the electron PADs (Figure 1h) were volatile inside the FR, the electron PADs around the current layer (the pink region in Figure 1) did not change dramatically while crossing the current sheet. And the bipolar signature of the FR was mainly observed in the component normal to the magnetotail current sheet (Z-GSE). These indicate that the reconnecting current sheet was indeed observed at the center of the FR. However, unlike at the magnetopause, the plasma conditions were uniform in the magnetotail. There was a slight possibility that similar electron PADs were observed in two unconnected flux tubes. Thus, we still cannot entirely exclude the possibility of two interlinked flux tubes.

The compression by ion bulk flow at the center of the FR was a potential explanation for the formation of reconnecting current layer. Due to the strong compression, the oppositely poloidal magnetic field (B_z) lines met at the center of the FR, and then the magnetic reconnection could be enabled. When the poloidal magnetic fields were reconnected, the initial magnetic field topology could change, and the initial FR may divide into two secondary FRs, as illustrated in Figure 4. The division of FR via reconnection may be hard because the strong magnetic tension force would suppress this process. However, a recent 2-D Hybrid-Vlasov simulation indeed found that the ion-scale FR could divide into two or even three smaller FRs via reconnection (Akhavan-Tafti et al., 2020). How to overcome the magnetic tension force to form a reconnecting current sheet is still unclear. The compression by plasma flow is a possible mechanism, but further study is needed to reveal the exact mechanism. Moreover, a recent observation also found that strong energy dissipation could occur at the center of the FR in the magnetotail (Huang et al., 2019), but the mechanism was unclear. It suggests that the instabilities can be easily excited inside the FRs, as they are propagating in the magnetotail current sheet.

The reconnecting current sheet could also be found at the center of the FRs formed by the coalescence of FRs. This process has been studied extensively in numerical simulations (Cazzola et al., 2015; Finn & Kaw, 1977; Oka et al., 2010; Pritchett, 2007) and observations (R. S. Wang et al., 2016, 2017; Zhao, Wang, Lu, et al., 2016; Zhou et al., 2017). The direction of the reconnecting current sheet during the coalescence should be anti-parallel to the background current of the FR, which was different from our observation. Thus, it can be ruled out that the current sheet was formed by the coalescence of FRs in our work. However, a simulation found that the coalescing FRs could bounce (Karimabadi et al., 2011), resulting in a "pull current sheet" between FRs that were not currently coalescing. The direction of the "pull current sheet" was parallel to the background current of the FRs, similar to our observation. So it was also a possible explanation for our observation. However, it requires that the coalescing FRs arrange in the Z-GSE direction, which is rarely observed in the magnetotail. Thus, it is more likely that this reconnecting current sheet was caused by the division of FR.

The FR with a magnetic field depression at its center is called crater-shaped FR, which has previously been proposed to be in an early stage of the formation of FR (Zhang et al., 2010) or the results of the back-and-forth crossing of a typical FR (Owen et al., 2008). In our event, the decrease of B_M, the hall magnetic field, supported the depression of the magnitude of the magnetic field, indicating that the hall magnetic field generated by the magnetic reconnection at the center of the FR could also produce the crater-shaped FR.

In conclusion, we report a crater-shaped FR embedded in an unstable tailward plasma flow in the magnetotail. Due to the strong compression by ions bulk flow, a reconnection current layer with a strong guide field formed at the center of the FR. The reconnecting current layer could change the magnetic field topology of the initial FR and divide the initial FR into two secondary FRs.

Data Availability Statement

All the MMS data used in this work are available at the MMS data center (https://lasp.colorado.edu/mms/sdc/public/about/browse-wrapper/).

Acknowledgments
This work is supported by the B-type Strategic Priority Program of the Chinese Academy of Sciences (XDB41000000), the National Science Foundation of China (NSFC) Grants (41922030, 42174181, and 42174187), key research program of frontier sciences CAS (QYZDJ-SSW-DQC010), and the Fundamental Research Funds for the Central Universities. We thank the entire MMS team and instrument principal investigators for providing and calibrating data.

References

Akhavan-Tafti, M., Palmroth, M., Slavin, J. A., Battarbee, M., Ganse, U., Grandin, M., et al. (2020). Comparative analysis of the vlasiator simulations and MMS observations of multiple X-line reconnection and flux transfer events. *Journal of Geophysical Research: Space Physics*, *125*(7), e2019JA027410. https://doi.org/10.1029/2019JA027410

Bhattacharjee, A., Huang, Y. M., Yang, H., & Rogers, B. (2009). Fast reconnection in high-Lundquist-number plasmas due to the plasmoid instability. *Physics of Plasmas*, *16*(11), 112102. https://doi.org/10.1063/1.3264103

Burch, J. L., Moore, T. E., Torbert, R. B., & Giles, B. L. (2016). Magnetospheric multiscale overview and science objectives. *Space Science Reviews*, *199*(1–4), 5–21. https://doi.org/10.1007/s11214-015-0164-9

Burch, J. L., Torbert, R. B., Phan, T. D., Chen, L. J., Moore, T. E., Ergun, R. E., et al. (2016). Electron-scale measurements of magnetic reconnection in space. *Science*, *352*(6290), aaf2939. https://doi.org/10.1126/science.aaf2939

Cazzola, E., Innocenti, M. E., Markidis, S., Goldman, M. V., Newman, D. L., & Lapenta, G. (2015). On the electron dynamics during island coalescence in asymmetric magnetic reconnection. *Physics of Plasmas*, *22*(9), 092901. https://doi.org/10.1063/1.4929847

Chen, L. J., Bhattacharjee, A., Puhl-Quinn, P. A., Yang, H., Bessho, N., Imada, S., et al. (2008). Observation of energetic electrons within magnetic islands. *Nature Physics*, *4*(1), 19–23. https://doi.org/10.1038/nphys777

Chen, Z. Z., Fu, H. S., Wang, T. Y., Cao, D., Peng, F. Z., Yang, J., & Xu, Y. (2019). Reconstructing the flux-rope topology using the FOTE method. *Science China Technological Sciences*, *62*(1), 144–150. https://doi.org/10.1007/s11431-017-9201-1

Daughton, W., Roytershteyn, V., Albright, B. J., Karimabadi, H., Yin, L., & Bowers, K. J. (2009). Transition from collisional to kinetic regimes in large-scale reconnection layers. *Physical Review Letters*, *103*(6), 065004. https://doi.org/10.1103/PhysRevLett.103.065004

Daughton, W., Roytershteyn, V., Karimabadi, H., Yin, L., Albright, B. J., Bergen, B., & Bowers, K. J. (2011). Role of electron physics in the development of turbulent magnetic reconnection in collisionless plasmas. *Nature Physics*, *7*(7), 539–542. https://doi.org/10.1038/Nphys1965

Deng, X. H., & Matsumoto, H. (2001). Rapid magnetic reconnection in the Earth's magnetosphere mediated by whistler waves. *Nature*, *410*(6828), 557–560. https://doi.org/10.1038/35069018

Drake, J. F., Swisdak, M., Che, H., & Shay, M. A. (2006). Electron acceleration from contracting magnetic Islands during reconnection. *Nature*, *443*(7111), 553–556. https://doi.org/10.1038/nature05116

Eastwood, J. P., Phan, T. D., Cassak, P. A., Gershman, D. J., Haggerty, C., Malakit, K., et al. (2016). Ion-scale secondary flux ropes generated by magnetopause reconnection as resolved by MMS. *Geophysical Research Letters*, *43*(10), 4716–4724. https://doi.org/10.1002/2016gl068747

Eastwood, J. P., Sibeck, D. G., Slavin, J. A., Goldstein, M. L., Lavraud, B., Sitnov, M., et al. (2005). Observations of multiple X-line structure in the Earth's magnetotail current sheet: A cluster case study. *Geophysical Research Letters*, *32*(11), L11105. https://doi.org/10.1029/2005gl022509

Ergun, R. E., Tucker, S., Westfall, J., Goodrich, K. A., Malaspina, D. M., Summers, D., et al. (2016). The axial double probe and fields signal processing for the MMS mission. *Space Science Reviews*, *199*(1–4), 167–188. https://doi.org/10.1007/s11214-014-0115-x

Fargette, N., Lavraud, B., Oieroset, M., Phan, T. D., Toledo-Redondo, S., Kieokaew, R., et al. (2020). On the ubiquity of magnetic reconnection inside flux transfer event-like structures at the Earth's magnetopause. *Geophysical Research Letters*, *47*(6), e2019GL086726. https://doi.org/10.1029/2019GL086726

Finn, J. M., & Kaw, P. K. (1977). Coalescence instability of magnetic islands. *Physics of Fluids*, *20*(1), 72–78. https://doi.org/10.1063/1.861709

Fu, X. R., Lu, Q. M., & Wang, S. (2006). The process of electron acceleration during collisionless magnetic reconnection. *Physics of Plasmas*, *13*(1), 012309. https://doi.org/10.1063/1.2164808

Hasegawa, H., Wang, J., Dunlop, M. W., Pu, Z. Y., Zhang, Q. H., Lavraud, B., et al. (2010). Evidence for a flux transfer event generated by multiple X-line reconnection at the magnetopause. *Geophysical Research Letters*, *37*(16), L16101. https://doi.org/10.1029/2010gl044219

Huang, C., Lu, Q. M., Wang, R. S., Guo, F., Wu, M. Y., Lu, S., & Wang, S. (2017). Development of turbulent magnetic reconnection in a magnetic island. *The Astrophysical Journal*, *835*(2), 245. https://doi.org/10.3847/1538-4357/835/2/245

Huang, S. Y., Jiang, K., Yuan, Z. G., Zhou, M., Sahraoui, F., Fu, H. S., et al. (2019). Observations of flux ropes with strong energy dissipation in the magnetotail. *Geophysical Research Letters*, *46*(2), 580–589. https://doi.org/10.1029/2018gl081099

Huang, S. Y., Sahraoui, F., Retino, A., Le Contel, O., Yuan, Z. G., Chasapis, A., et al. (2016). MMS observations of ion-scale magnetic island in the magnetosheath turbulent plasma. *Geophysical Research Letters*, *43*(15), 7850–7858. https://doi.org/10.1002/2016gl070033

Huba, J. D. (2005). Hall magnetic reconnection: Guide field dependence. *Physics of Plasmas*, *12*(1), 012322. https://doi.org/10.1063/1.1834592

Hwang, K. J., Dokgo, K., Choi, E., Burch, J. L., Sibeck, D. G., Giles, B. L., et al. (2020). Magnetic reconnection inside a flux rope induced by Kelvin-Helmholtz vortices. *Journal of Geophysical Research: Space Physics*, *125*(4), e2019JA027665. https://doi.org/10.1029/2019JA027665

Hwang, K. J., Sibeck, D. G., Giles, B. L., Pollock, C. J., Gershman, D., Avanov, L., et al. (2016). The substructure of a flux transfer event observed by the MMS spacecraft. *Geophysical Research Letters*, *43*(18), 9434–9443. https://doi.org/10.1002/2016gl070934

Kacem, I., Jacquey, C., Genot, V., Lavraud, B., Vernisse, Y., Marchaudon, A., et al. (2018). Magnetic reconnection at a thin current sheet separating two interlaced flux tubes at the Earth's magnetopause. *Journal of Geophysical Research: Space Physics*, *123*(3), 1779–1793. https://doi.org/10.1002/2017ja024537

Karimabadi, H., Dorelli, J., Roytershteyn, V., Daughton, W., & Chacon, L. (2011). Flux pileup in collisionless magnetic reconnection: Bursty interaction of large flux ropes. *Physical Review Letters*, *107*(2), 025002. https://doi.org/10.1103/PhysRevLett.107.025002

Kieokaew, R., Lavraud, B., Foullon, C., Toledo-Redondo, S., Fargette, N., Hwang, K., et al. (2020). Magnetic reconnection inside a flux transfer event-like structure in magnetopause Kelvin-Helmholtz waves. *Journal of Geophysical Research: Space Physics*, *125*(6), e2019JA027527. https://doi.org/10.1029/2019JA027527

Labelle, J., Treumann, R. A., Haerendel, G., Bauer, O. H., Paschmann, G., Baumjohann, W., et al. (1987). Ampte IRM observations of waves associated with flux-transfer events in the magnetosphere. *Journal of Geophysical Research*, *92*(A6), 5827–5843. https://doi.org/10.1029/JA092iA06p05827

Lapenta, G., Markidis, S., Goldman, M. V., & Newman, D. L. (2015). Secondary reconnection sites in reconnection-generated flux ropes and reconnection fronts. *Nature Physics*, *11*(8), 690–695. https://doi.org/10.1038/Nphys3406

Lee, L., & Fu, Z. (1985). A theory of magnetic flux transfer at the Earth's magnetopause. *Geophysical Research Letters*, *12*(2), 105–108. https://doi.org/10.1029/gl012i002p00105

Li, X. M., Wang, R. S., Lu, Q. M., Hwang, Y. O. O., Zong, Q. G., Russell, C. T., & Wang, S. (2019). Observation of nongyrotropic electron distribution across the electron diffusion region in the magnetotail reconnection. *Geophysical Research Letters*, *46*(24), 14263–14273. https://doi.org/10.1029/2019gl085014

Lindqvist, P. A., Olsson, G., Torbert, R. B., King, B., Granoff, M., Rau, D., et al. (2016). The spin-plane double probe electric field instrument for MMS. *Space Science Reviews*, *199*(1–4), 137–165. https://doi.org/10.1007/s11214-014-0116-9

Loureiro, N. F., Schekochihin, A. A., & Cowley, S. C. (2007). Instability of current sheets and formation of plasmoid chains. *Physics of Plasmas*, *14*(10), 100703. https://doi.org/10.1063/1.2783986

Øieroset, M., Phan, T., Eastwood, J., Fujimoto, M., Daughton, W., Shay, M., et al. (2011). Direct evidence for a three-dimensional magnetic flux rope flanked by two active magnetic reconnection X lines at Earth's magnetopause. *Physical Review Letters*, *107*(16), 165007. https://doi.org/10.1103/physrevlett.107.165007

Øieroset, M., Phan, T. D., Drake, J. F., Eastwood, J. P., Fuselier, S. A., Strangeway, R. J., et al. (2019). Reconnection with magnetic flux pileup at the interface of converging jets at the magnetopause. *Geophysical Research Letters*, *46*(4), 1937–1946. https://doi.org/10.1029/2018gl080994

Øieroset, M., Phan, T. D., Haggerty, C., Shay, M. A., Eastwood, J. P., Gershman, D. J., et al. (2016). MMS observations of large guide field symmetric reconnection between colliding reconnection jets at the center of a magnetic flux rope at the magnetopause. *Geophysical Research Letters*, *43*(11), 5536–5544. https://doi.org/10.1002/2016gl069166

Oka, M., Phan, T. D., Krucker, S., Fujimoto, M., & Shinohara, I. (2010). Electron acceleration by multi-island coalescence. *The Astrophysical Journal*, *714*(1), 915–926. https://doi.org/10.1088/0004-637x/714/1/915

Owen, C. J., Marchaudon, A., Dunlop, M. W., Fazakerley, A. N., Bosqued, J. M., Dewhurst, J. P., et al. (2008). Cluster observations of "crater" flux transfer events at the dayside high-latitude magnetopause. *Journal of Geophysical Research*, *113*(A7), A07S04. https://doi.org/10.1029/2007ja012701

Pollock, C., Moore, T., Jacques, A., Burch, J., Gliese, U., Saito, Y., et al. (2016). Fast plasma investigation for magnetospheric multiscale. *Space Science Reviews*, *199*(1–4), 331–406. https://doi.org/10.1007/s11214-016-0245-4

Pritchett, P. L. (2007). Kinetic properties of magnetic merging in the coalescence process. *Physics of Plasmas*, *14*(5), 052102. https://doi.org/10.1063/1.2727458

Pritchett, P. L., & Coroniti, F. V. (2004). Three-dimensional collisionless magnetic reconnection in the presence of a guide field. *Journal of Geophysical Research*, *109*(A1), A01220. https://doi.org/10.1029/2003ja009999

Ricci, P., Brackbill, J. U., Daughton, W., & Lapenta, G. (2004). Collisionless magnetic reconnection in the presence of a guide field. *Physics of Plasmas*, *11*(8), 4102–4114. https://doi.org/10.1063/1.1768552

Russell, C. T., Anderson, B. J., Baumjohann, W., Bromund, K. R., Dearborn, D., Fischer, D., et al. (2016). The magnetospheric multiscale magnetometers. *Space Science Reviews*, *199*(1–4), 189–256. https://doi.org/10.1007/s11214-014-0057-3

Russell, C. T., & Elphic, R. C. (1978). Initial ISEE magnetometer results—magnetopause observations. *Space Science Reviews*, *22*(6), 681–715. https://doi.org/10.1007/bf00212619

Russell, C. T., & Qi, Y. (2020). Flux ropes are born in pairs: An outcome of interlinked, reconnecting flux tubes. *Geophysical Research Letters*, *47*(15), e2020GL087620. https://doi.org/10.1029/2020GL087620

Samtaney, R., Loureiro, N. F., Uzdensky, D. A., Schekochihin, A. A., & Cowley, S. C. (2009). Formation of plasmoid chains in magnetic reconnection. *Physical Review Letters*, *103*(10), 105004. https://doi.org/10.1103/PhysRevLett.103.105004

Scholer, M. (1988). Magnetic-flux transfer at the magnetopause based on single X-line bursty reconnection. *Geophysical Research Letters*, *15*(4), 291–294. https://doi.org/10.1029/GL015i004p00291

Schwartz, S. J. (1998). Shock and discontinuity normals, mach numbers, and related parameters. *ISSI Scientific Reports Series*, *1*, 249–270.

Sibeck, D. G., Siscoe, G. L., Slavin, J. A., Smith, E. J., Bame, S. J., & Scarf, F. L. (1984). Magnetotail flux ropes. *Geophysical Research Letters*, *11*(10), 1090–1093. https://doi.org/10.1029/GL011i010p01090

Slavin, J. A., Lepping, R. P., Gjerloev, J., Fairfield, D. H., Hesse, M., Owen, C. J., et al. (2003). Geotail observations of magnetic flux ropes in the plasma sheet. *Journal of Geophysical Research*, *108*(A1), 1015. https://doi.org/10.1029/2002ja009557

Sonnerup, B. U., & Scheible, M. (1998). Minimum and maximum variance analysis. *Analysis Methods for Multi-Spacecraft Data*, *1*, 185–220.

Teh, W. L., Denton, R. E., Sonnerup, B. U. O., & Pollock, C. (2017). MMS observations of oblique small-scale magnetopause flux ropes near the ion diffusion region during weak guide-field reconnection. *Geophysical Research Letters*, *44*(13), 6517–6524. https://doi.org/10.1002/2017gl074291

Torbert, R. B., Burch, J. L., Phan, T. D., Hesse, M., Argall, M. R., Shuster, J., et al. (2018). Electron-scale dynamics of the diffusion region during symmetric magnetic reconnection in space. *Science*, *362*(6421), 1391–1395. https://doi.org/10.1126/science.aat2998

Wang, R. S., Lu, Q., Nakamura, R., Baumjohann, W., Russell, C. T., Burch, J. L., et al. (2017). Interaction of magnetic flux ropes via magnetic reconnection observed at the magnetopause. *Journal of Geophysical Research: Space Physics*, *122*(10), 10436–10447. https://doi.org/10.1002/2017ja024482

Wang, R. S., Lu, Q. M., Du, A. M., & Wang, S. (2010). In situ observations of a secondary magnetic island in an ion diffusion region and associated energetic electrons. *Physical Review Letters*, *104*(17), 175003. https://doi.org/10.1103/PhysRevLett.104.175003

Wang, R. S., Lu, Q. M., Li, X., Huang, C., & Wang, S. (2010). Observations of energetic electrons up to 200 keV associated with a secondary island near the center of an ion diffusion region: A cluster case study. *Journal of Geophysical Research*, *115*(A11), A11201. https://doi.org/10.1029/2010ja015473

Wang, R. S., Lu, Q. M., Lu, S., Russell, C. T., Burch, J. L., Gershman, D. J., et al. (2020). Physical implication of two types of reconnection electron diffusion regions with and without ion-coupling in the magnetotail current sheet. *Geophysical Research Letters*, *47*(21), e2020GL088761. https://doi.org/10.1029/2020GL088761

Wang, R. S., Lu, Q. M., Nakamura, R., Huang, C., Du, A. M., Guo, F., et al. (2016). Coalescence of magnetic flux ropes in the ion diffusion region of magnetic reconnection. *Nature Physics*, *12*(3), 263–267. https://doi.org/10.1038/Nphys3578

Wang, S. M., Wang, R. S., Lu, Q. M., Burch, J. L., & Wang, S. (2021). Energy dissipation via magnetic reconnection within the coherent structures of the magnetosheath turbulence. *Journal of Geophysical Research: Space Physics*, *126*(4), e2020JA028860. https://doi.org/10.1029/2020JA028860

Wang, S. M., Wang, R. S., Lu, Q. M., Fu, H. S., & Wang, S. (2020). Direct evidence of secondary reconnection inside filamentary currents of magnetic flux ropes during magnetic reconnection. *Nature Communications*, *11*(1), 3964. https://doi.org/10.1038/s41467-020-17803-3

Xia, Q., & Zharkova, V. (2018). Particle acceleration in coalescent and squashed magnetic Islands I. Test particle approach. *Astronomy & Astrophysics*, *620*, A121. https://doi.org/10.1051/0004-6361/201833599

Yao, S. T., Shi, Q. Q., Guo, R. L., Yao, Z. H., Fu, H. S., Degeling, A. W., et al. (2020). Kinetic-scale flux rope in the magnetosheath boundary layer. *The Astrophysical Journal*, *897*(2), 137. https://doi.org/10.3847/1538-4357/ab9620

Zenitani, S., Hesse, M., Klimas, A., & Kuznetsova, M. (2011). New measure of the dissipation region in collisionless magnetic reconnection. *Physical Review Letters*, *106*(19), 195003. https://doi.org/10.1103/PhysRevLett.106.195003

Zhang, H., Kivelson, M. G., Khurana, K. K., McFadden, J., Walker, R. J., Angelopoulos, V., et al. (2010). Evidence that crater flux transfer events are initial stages of typical flux transfer events. *Journal of Geophysical Research*, *115*(A8), A08229. https://doi.org/10.1029/2009ja015013

Zhao, Y., Wang, R., Lu, Q. M., Du, A. M., Yao, Z. H., & Wu, M. Y. (2016). Coalescence of magnetic flux ropes observed in the tailward high-speed flows. *Journal of Geophysical Research: Space Physics*, *121*(11), 10898–10909. https://doi.org/10.1002/2016ja023526

Zhao, Y., Wang, R. S., & Du, A. M. (2016). Characteristics of field-aligned currents associated with magnetic flux ropes in the magnetotail: A statistical study. *Journal of Geophysical Research: Space Physics*, *121*(4), 3264–3277. https://doi.org/10.1002/2015ja022144

Zhong, J., Pu, Z. Y., Dunlop, M. W., Bogdanova, Y. V., Wang, X. G., Xiao, C. J., et al. (2013). Three-dimensional magnetic flux rope structure formed by multiple sequential X-line reconnection at the magnetopause. *Journal of Geophysical Research: Space Physics*, *118*(5), 1904–1911. https://doi.org/10.1002/jgra.50281

Zhong, Z. H., Zhou, M., Tang, R., Deng, X., Turner, D., Cohen, I., et al. (2020). Direct evidence for electron acceleration within ion-scale flux rope. *Geophysical Research Letters*, *47*(1), e2019GL085141. https://doi.org/10.1029/2019GL085141

Zhou, M., Berchem, J., Walker, R., El-Alaoui, M., Deng, X., Cazzola, E., et al. (2017). Coalescence of macroscopic flux ropes at the subsolar magnetopause: Magnetospheric multiscale observations. *Physical Review Letters*, *119*(5), 055101. https://doi.org/10.1103/PhysRevLett.119.055101

Zong, Q. G., Fritz, T. A., Pu, Z. Y., Fu, S. Y., Baker, D. N., Zhang, H., & Reme, H. (2004). Cluster observations of earthward flowing plasmoid in the tail. *Geophysical Research Letters*, *31*(18), L18803. https://doi.org/10.1029/2004gl020692